

Radial stretch reveals distinct populations of mechanosensitive mammalian somatosensory neurons

Martha R. C. Bhattacharya^{a,1}, Diana M. Bautista^{b,1,2}, Karin Wu^b, Henry Haebler^{a,c}, Ellen A. Lumpkin^{c,2}, and David Julius^{a,2}

^aDepartment of Physiology, University of California, San Francisco CA 94158; ^bDepartment of Molecular and Cell Biology, University of California, Berkeley CA 94720; and ^cDepartments of Neuroscience, Molecular Physiology and Biophysics, and Molecular and Human Genetics, Baylor College of Medicine, Houston, TX 77030

Contributed by David Julius, October 27, 2008 (sent for review October 4, 2008)

Primary afferent somatosensory neurons mediate our sense of touch in response to changes in ambient pressure. Molecules that detect and transduce thermal stimuli have been recently identified, but mechanisms underlying mechanosensation, particularly in vertebrate organisms, remain enigmatic. Traditionally, mechanically evoked responses in somatosensory neurons have been assessed one cell at a time by recording membrane currents in response to application of focal pressure, suction, or osmotic challenge. Here, we used radial stretch in combination with live-cell calcium imaging to gain a broad overview of mechanosensitive neuronal subpopulations. We found that different stretch intensities activate distinct subsets of sensory neurons as defined by size, molecular markers, or pharmacological attributes. In all subsets, stretch-evoked responses required extracellular calcium, indicating that mechanical force triggers calcium influx. This approach extends the repertoire of stimulus paradigms that can be used to examine mechanotransduction in mammalian sensory neurons, facilitating future physiological and pharmacological studies.

mechanotransduction | sensory signaling | somatosensation | touch

Mechanotransduction regulates myriad physiological processes in mammals, including blood pressure regulation, bladder voiding, and stretch-evoked responses of other visceral and vascular organs. Mechanotransduction also represents an important component of our exterosensory repertoire, where it is essential for auditory and somatosensory function (1–5). In somatosensory neurons, this pertains to the detection of both innocuous and noxious mechanical stimuli that underlie our sense of touch, proprioception, and pain (6, 7).

Detection of mechanical forces by the somatosensory system is carried out by primary afferent neurons within trigeminal (TG) or dorsal root ganglia (DRG). Electrophysiological recordings from sensory nerve fibers suggest that mammalian mechanoreceptors can be classified into a variety of functionally distinct subgroups, depending on their threshold sensitivities and rates of adaptation (8, 9). When dissociated and placed in culture, TG or DRG neurons retain many aspects of their native function, including sensitivity to a range of physical and chemical stimuli (10). As such, membrane currents or calcium responses have been recorded from the somata of sensory neurons in response to a variety of mechanical challenges, such as suction, focal displacement of the cell surface, or stretch resulting from changes in osmolarity (11–17). Such analyses suggest that mechanical stimulation of sensory neurons activates cation-permeable channels that differ in their sensitivity to pressure and therefore define low and high threshold subpopulations that presumably contribute to detection of innocuous and noxious stimuli, respectively. Although these studies provide initial information about the nature of somatosensory responses to mechanical stimuli, each has its limitations that reflect difficulty in sampling large numbers of functionally and anatomically diverse cell types, and uncertainties as to whether any one experimental stimulus recapitulates physiological forces that

activate nerve endings in vivo. As such, there is a need to apply other paradigms to the analysis of sensory mechanotransduction, particularly those that offer the possibility of examining large numbers of cells while delivering a stimulus that is graded, uniform, and reproducible. Such systems offer the possibility of obtaining a broad overview of mechanosensitivity based on the analysis of thousands of individual neurons. They also open up the possibility of using high throughput analysis for the purpose of identifying molecules or pharmacological probes that contribute to or modulate the mechanotransduction machinery in sensory neurons or other mechanically sensitive cell types.

To address these issues, we have adapted radial stretch-based stimulation (18–20) for the analysis of mechanosensitivity in primary afferent neurons from mouse sensory ganglia. In this system, which has typically been used to study stretch-evoked responses in nonneural cells, dissociated neurons from DRG or TG are grown on flexible silicon membranes that can be distended by using calibrated vacuum pressure. Consequent responses can be detected on a population-wide basis by monitoring changes in intracellular free calcium. By using this approach, we observe a distinct subset of trigeminal neurons that respond to relatively low threshold stretch stimuli, followed by recruitment of additional responders as the stimulus magnitude increases. Interestingly, stretch-responsive neurons represent a subset of those responding to hypotonic-induced swelling, suggesting that these stimulus paradigms do not activate equivalent physiological responses. Moreover, neurons responding to low threshold radial stretch also respond to hydroxy- α -sanshool, the pungent ingredient in Szechuan peppers that excites a population of large-diameter, TrkC-expressing cells that includes presumptive light touch receptors and proprioceptors (21). In summary, these findings show that radial stretch is a viable and physiologically relevant method for analyzing mechanically evoked responses of somatosensory neurons on a population wide basis.

Results

Simultaneous calcium imaging and stretch has been used to visualize mechanosensory responses in cultured smooth muscle cells (19). We therefore adopted this approach to the analysis of cultured sensory neurons isolated from mouse DRG or TG. Dissociated neurons were plated on thin silicone discs coated with laminin, allowed to adhere overnight, loaded with calcium-

Author contributions: M.R.C.B., D.B., E.A.L., and D.J. designed research; M.R.C.B., D.B., and K.W. performed research; M.R.C.B., D.B., and H.H. contributed new reagents/analytic tools; M.R.C.B., D.B., E.A.L., and D.J. analyzed data; and M.R.C.B., D.B., and D.J. wrote the paper.

The authors declare no conflict of interest.

¹M.R.C.B. and D.M.B. contributed equally to this work.

²To whom correspondence may be addressed. E-mail: julius@cmp.ucsf.edu, lumpkin@bcm.tmc.edu, or dbautista@berkeley.edu.

This article contains supporting information online at www.pnas.org/cgi/content/full/0810801105/DCSupplemental.

© 2008 by The National Academy of Sciences of the USA

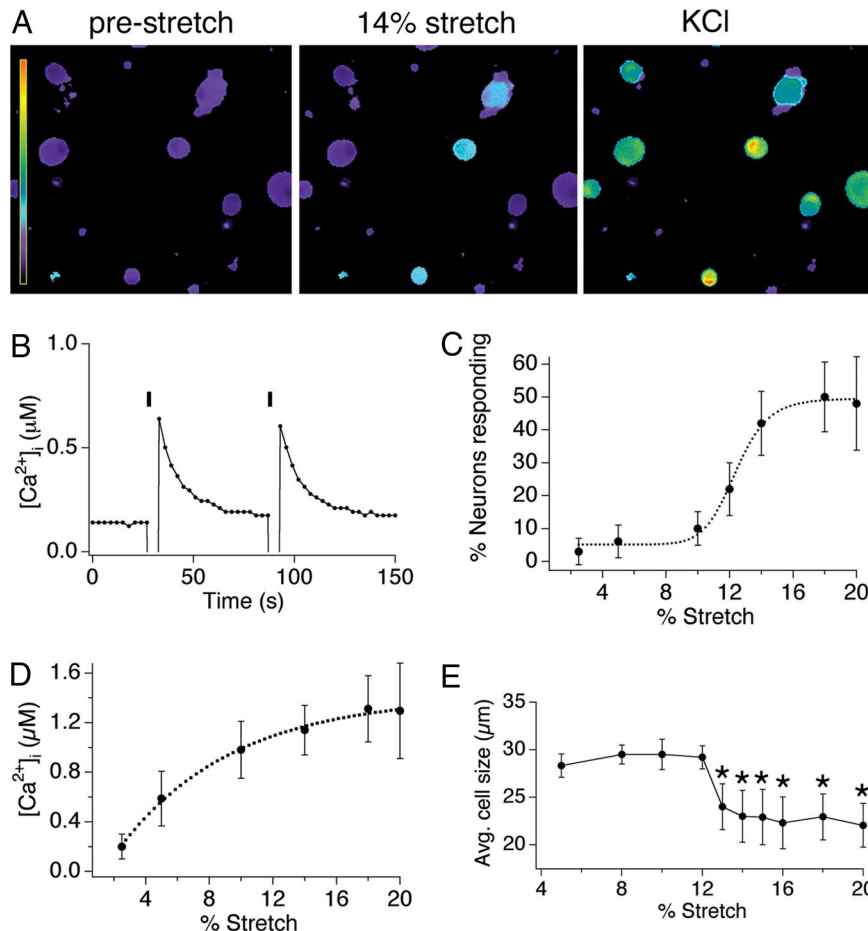


Fig. 1. Radial stretch activates a subset of trigeminal sensory neurons. (A) Calcium responses of dissociated mouse trigeminal neurons to 14% radial stretch (Middle) and 140 mM KCl Ringer's solution (Right). Scale bar indicates the intracellular calcium concentration, ranging from 0.1 to 4 μM $[\text{Ca}^{2+}]_i$. (B) Calcium response in a representative cell to two applications of a 14% radial stretch stimulus. (C) Dose–response curve displaying the percentage of neurons activated by varying magnitudes of stretch. (D) Dose–response curve displaying the magnitude of the calcium response triggered by varying magnitudes of stretch. (E) The mean diameter of responding neurons is plotted versus stretch magnitude. For all experiments, $n \geq 200$ cells per point, obtained from a minimum of three different neuronal preparations. All data are reported as means \pm SEM.

sensitive dye (Fura-2), and transferred to a vacuum driven stretch chamber. In this system, the magnitude of the stretch stimulus was calibrated by visualizing stretch-evoked changes in the distance between fluorescent beads affixed to the membrane [supporting information (SI) Fig. S1], providing a linear dose–response curve between 2 and 20% radial stretch, which corresponded to a radial movement of 3.5–40.2 μm . Stretch stimuli were generally applied for a 2-s period taking into account several experimental parameters. First, peak stretch was reached within 0.7 sec, irrespective of stretch intensity. Second, stretch was accompanied by membrane displacement and subsequent relaxation over a period of 2–5 s, causing a focal plane change that transiently precluded cellular imaging. While the response to stretch peaked during this blackout period, we were able to image the falling phase of the calcium response as a measure of stretch-evoked activity. Thus, a 2-s stretch duration was chosen to maximize the stimulus and minimize the blackout period whereas capturing the majority of the cellular response.

Application of a 2-s stretch over a range of stimulus intensities evoked a transient rise in intracellular calcium among a subset of cultured neonatal trigeminal mouse neurons (Fig. 1A). During the initial blackout period we were unable to visualize the rising phase of the response (note the stimulus artifact), but stimulus-dependent increases in intracellular calcium that decayed exponentially to prestimulus calcium levels were elicited repetitively

with successive applications of stretch (Fig. 1B and Movie S1). Taken together, these data show that radial stretch elicits bona fide calcium increases that correspond to physiologic responses, rather than nonspecific injury leading to loss of cell integrity.

Dose–response analysis revealed that both the percentage of neurons activated by stretch (responders) and the magnitude of the response increased with stretch intensity (Fig. 1C and D). For example, $6.1 \pm 5\%$ of neurons responded to 5% stretch stimuli with an average peak calcium concentration of $0.58 \pm 0.22 \mu\text{M}$, whereas $48 \pm 14.2\%$ of neurons responded to 20% stretch stimuli with an average peak calcium concentration of $1.3 \pm 0.38 \mu\text{M}$ ($P < 0.01$, one-way ANOVA). Additionally, neurons binned into two main anatomical classes such that those showing sensitivity to low stretch intensity had relatively large soma diameters ($28 \pm 2.7 \mu\text{m}$), whereas those responding only at higher magnitudes were significantly smaller ($23 \pm 1.4 \mu\text{m}$; $P < 0.05$, one-way ANOVA) (Fig. 1E). In this regard, 12% stretch represents the approximate demarcation point between these two classes of low versus high threshold responders (Fig. 1E). Similar responses were also observed with neonatal or adult DRG neurons (data not shown).

To further characterize the responses of these two populations over the full range of stimulus intensities, we recorded responses of individual neurons to repetitive stretch stimuli of increasing magnitude. Low threshold cells responded to all magnitudes with

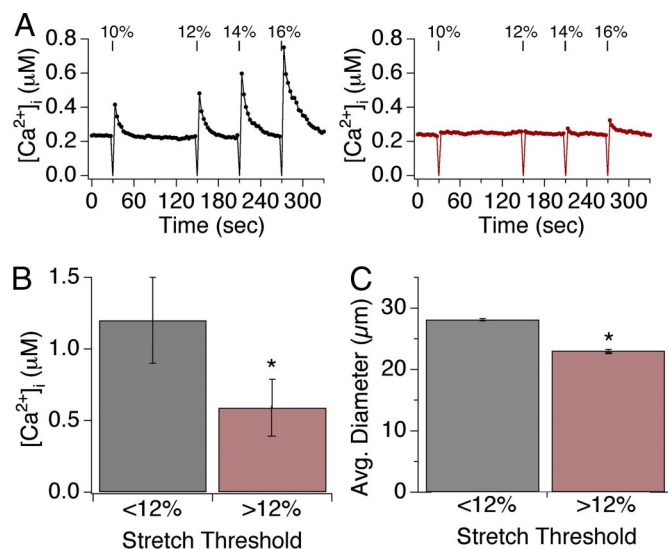


Fig. 2. Two subsets of sensory neurons display varying sensitivity to stretch. (A) Representative responses of individual neurons to four subsequent applications of radial stretch 10, 12, 14, and 16%. Low-threshold neurons respond to all magnitudes of stretch (black, *Left graph*), whereas a high-threshold neuron responded only to stretch magnitudes $\geq 12\%$ (red, *Right graph*). (B) Low-threshold neurons displayed significantly larger peak calcium transients in response to all levels of stretch versus those observed in high-threshold neurons. (C) Neurons showing sensitivity to low stretch intensity had relatively large soma diameters ($28 \pm 2.7 \mu\text{m}$), whereas those responding only at higher magnitudes were significantly smaller ($23 \pm 1.4 \mu\text{m}$; $P < 0.05$, one-way ANOVA). Asterisks denotes $P < 0.05$; $n \geq 10$ trials/data point, with ≥ 30 neurons/trial.

continually increasing peak calcium levels as a function of stimulus intensity. High threshold responders displayed calcium transients that also increased as a function of stimulus intensity above the 12% stretch threshold (Fig. 2A and [Movie S2](#)). When averaging peak calcium signals in the high threshold group, we found that signals were of significantly lower magnitude compared with those of the low threshold group at all stimulus intensities (low: $1.2 \pm 0.31 \mu\text{M}$; High: $0.59 \pm 0.2 \mu\text{M}$; $P < 0.05$, one-way ANOVA (Fig. 2A and B).

To classify these populations of stretch-sensitive cells, we examined their responses to a variety of chemical irritants known to activate different subpopulations of primary afferent neurons (21, 22). Interestingly, low threshold neurons responded to hydroxy- α -sanshool, but not to capsaicin (the pungent agent from 'hot' chili peppers) (Fig. 3A). Thus, these neurons likely correspond to the population of large diameter, myelinated low-threshold mechanoreceptors that express the hydroxy- α -sanshool receptor, KCNK18, but not the capsaicin receptor, TRPV1. In contrast, high threshold neurons responded to both hydroxy- α -sanshool and capsaicin (Fig. 3B), likely corresponding to small diameter, unmyelinated nociceptors that express both KCNK18 and TRPV1. A subset ($\approx 50\%$) of capsaicin-sensitive cells expresses the mustard oil receptor, TRPA1, and release neuropeptides (CGRP and substance P) to generate neurogenic inflammation after excitation (23, 24). Interestingly, this group of mustard oil-sensitive, peptidergic neurons failed to respond to stretch (Fig. 3C), consistent with the previous observation that sanshool excites the nonpeptidergic subpopulation of capsaicin-sensitive nociceptors (21). Menthol activates a distinct subset of sensory neurons that express the cold-sensitive ion channel TRPM8 ($\approx 10\%$, data not shown and ref. 25). Menthol-sensitive cells did not respond to stretch, and likewise, stretch-sensitive cells did not express TRPM8 as determined by their lack of sensitivity to menthol (Fig. 3C). Finally, all stretch sensitive

neurons were activated by a hypotonic stimulus (220 mOsm) (Fig. 3C and D), which has also been used to identify mechanosensitive cells *in vitro* (11, 17, 26). Taken together, our results suggest that stretch-sensitive cells correspond to subpopulations of nonpeptidergic, unmyelinated C-fiber nociceptors, and myelinated A-fiber low-threshold mechanoreceptors.

Stretch-evoked calcium transients could result from calcium influx through cation channels, or via release from intracellular stores. To distinguish between these possibilities, we examined stretch-evoked responses when chelating all extracellular calcium with EGTA (2 mM). Under these conditions, stretch-evoked responses were abolished (Fig. 4A and D), demonstrating that stretch triggers calcium influx across the plasma membrane. The calcium transients that we observe could be produced by stretch-evoked membrane depolarization with subsequent opening of voltage-gated calcium channels. To address this possibility, we measured stretch-evoked responses in the presence of a mixture of voltage-gated calcium channel inhibitors that abolish calcium influx after membrane depolarization by high (75 mM) extracellular potassium (21). Under these same conditions, stretch-evoked responses were unaffected in regard to both prevalence and magnitude (Fig. 4B and D). The trivalent ion gadolinium (Gd^{3+}) blocks transduction channels in a variety of mechanosensitive cell types, including vascular smooth muscle and auditory hair cells, and bacterial stretch-activated MscL channels. Indeed, we found that application of Gd^{3+} caused complete block of stretch responses in sensory neurons (Fig. 3C and D). In contrast, ruthenium red, which serves as a pore blocker for some TRP (e.g., TRPV1, TRPV3, TRPV4, and TRPA1) and other cationic channels (27) had no effect on stretch-evoked responses (Fig. 4D). Taken together, these results demonstrate that stretch triggers calcium influx through a voltage-independent cation channel that is blocked by gadolinium, but not ruthenium red.

Discussion

Radial stretch has been widely used to stimulate cultured muscle cells as a paradigm for investigating both short- and long-term consequences of mechanical force (19, 28). In this study, we combine radial stretch with live cell calcium imaging to examine responses of cultured sensory neurons to mechanical stimuli. This technique offers a number of experimental advantages when compared with other types of mechanical challenges, such as focal displacement, suction, or pressure. First among these is the ability to deliver stimuli and monitor responses to a large cohort of cells, facilitating direct comparisons among sensory neuron subtypes under identical conditions, thereby facilitating quantitative population studies. Second, cells are readily accessible for pharmacologic manipulation and mechanical stimuli can be delivered over a wide and graded range of intensities, allowing for relatively detailed dose-response analysis. Third, the approach is relatively noninvasive compared with displacement- or suction-based methods, in which neurons often experience irreparable damage. Last, stretch elicits a mechanical stimulus across the entire region of cell-elastic membrane contact, which greatly exceeds the area stimulated by focal application of pressure or suction. While hypotonicity offers similar advantages compared with focal displacement or suction, there is still some debate as to whether cell swelling is an appropriate representation of the mechanical stimuli experienced by somatosensory neurons *in vivo*. In any case, the lack of complete overlap between hypotonic- and stretch-evoked responses suggests that different mechanisms come into play.

The obvious disadvantage of the stretch paradigm is the inability to simultaneously stretch cells and record membrane currents; however, modifications to the system may permit such simultaneous recordings at low levels of stretch, where substrate movement is minimized. Moreover, there is a limit to the amount

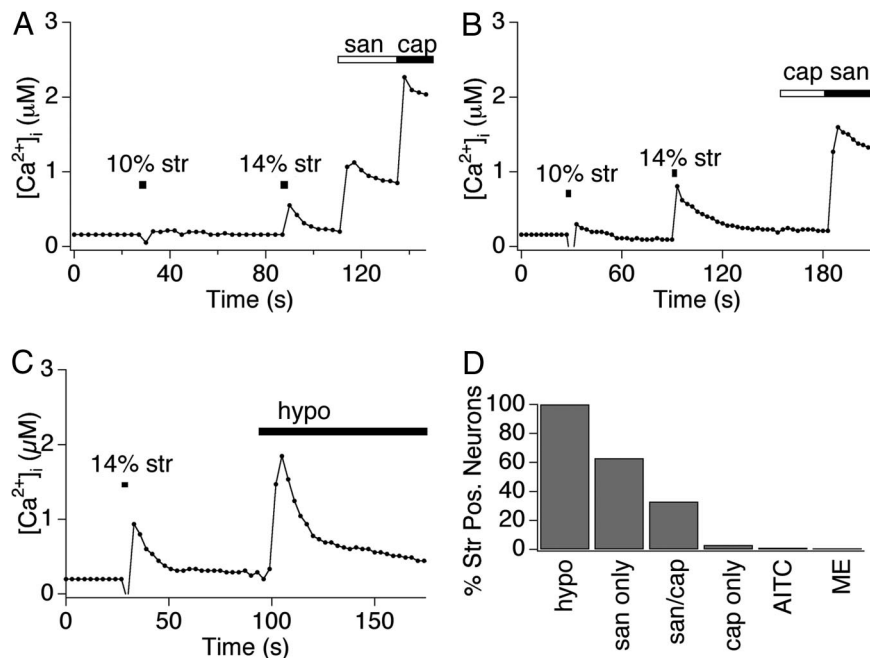


Fig. 3. Radial stretch excites presumptive nociceptors and mechanoreceptors. (A and B) Sensory neurons were stimulated by 10% stretch and 14% stretch stimuli, followed by application of capsaicin ($1 \mu\text{M}$) and hydroxy- α -sanshool ($100 \mu\text{M}$), and were analyzed by calcium imaging. Low threshold neurons are insensitive to capsaicin, but display hydroxy- α -sanshool sensitivity. High-threshold neurons are sensitive to both capsaicin and sanshool. (C) Sensory neurons were stimulated by 14% stretch followed by application of 30% hypoosmotic solution (220 mOsm). Both classes of neurons were sensitive to osmotic stimuli. However, only 70% of osmotic-sensitive neurons responded to radial stretch (data not shown). All traces displayed are responses observed in representative cells. (D) Quantitative analysis of concordance between stretch sensitivity and pharmacological attributes. Neurons displaying sensitivity to stretch were examined for activation by capsaicin (Cap; $1 \mu\text{M}$), hydroxy- α -sanshool (San; $100 \mu\text{M}$), mustard oil (AITC; $100 \mu\text{M}$), menthol (ME; $500 \mu\text{M}$), or hypotonic (Osmo; 220 mOsm) stimuli. Note the high (>95%) preponderance of stretch sensitivity among sanshool sensitive neurons, as compared with the relatively low ($\leq 2\%$) concordance between stretch sensitivity and mustard oil or menthol sensitivity.

of stretch that can be achieved with the current system ($\sim 20\%$ radial stretch) and thus we may not be detecting all mechanically sensitive cells, such as those with very high thresholds. Finally, there is the blackout period, during which data cannot be collected due to movement of the membrane during the stretch stimulus. Future improvements could involve the use of autofocus methods to collect images as the membrane moves to a different focal plane. Alternatively, one could generate a series of stacked images during the stretch stimulus such that ratio metric data can be collected at various positions along the z axis.

Taken together, our results define two main populations of stretch-sensitive neurons. The low threshold group responds to all stretch stimuli in a graded manner and includes neurons that respond to hydroxy- α -sanshool but not capsaicin. This cohort consists of medium- to large-diameter myelinated neurons that likely correspond to sensitive mechanoreceptors, including light touch receptors and proprioceptors (Fig. 5). By contrast, the high threshold group responds to stretch stimuli $>12\%$ in a graded manner, but with significantly lower magnitudes compared with the low threshold group. This cohort includes neurons that are sensitive to both sanshool and capsaicin, and likely correspond to a subpopulation of small-diameter, nonpeptidergic nociceptors that mediate the detection of more intense (noxious) mechanical stimuli. Interestingly, there remains a substantial cohort of neurons that are stretch-insensitive (at least within the range of stimulus intensities applied by our system). These include small-diameter, unmyelinated neurons that express the cold and menthol receptor, TRPM8, or the mustard oil receptor, TRPA1 (Fig. 5). These findings demonstrate the utility of the stretch-based paradigm for characterizing mechanically evoked responses in distinct subsets of somatosensory neurons.

Irrespective of differences in threshold sensitivity, all stretch-responsive neurons share some characteristics in common. For example, stretch promoted calcium influx in a manner that was independent of voltage-activated calcium channel activity, suggesting that stretch triggers the opening of a plasma membrane transduction channel with intrinsic permeability to calcium ions. Whether stretch activates this channel(s) directly or downstream of a secondary signaling pathway remains to be determined. In addition, responses were uniformly blocked by gadolinium, but not ruthenium red. Together, our pharmacological results suggest that radial-stretch evoked responses are not mediated by TRPA1 or by ruthenium-red-sensitive TRPV channels. This is corroborated by the fact that TG neurons from TRPA1, TRPV4, or TRPV1/TRPA1 double knockout mice displayed stretch-evoked responses that were indistinguishable (similar magnitude and prevalence) from those of wild type controls (Fig. S2).

In general, these findings are consistent with recent studies using focal pressure or suction to characterize mechanically evoked responses among cultured sensory neurons (13, 14). In each case, distinct populations of low and high threshold responders are similarly identified. Moreover, blockade by gadolinium is observed, irrespective of whether the stimulus is delivered by focal displacement, suction, or stretch. However, some notable differences do exist. For example, responses to displacement have been observed in both populations of capsaicin-sensitive cells, including mustard oil-sensitive peptidergic and mustard oil-insensitive, nonpeptidergic neurons. Moreover, some or all displacement-evoked responses were blocked by ruthenium red (14), which did not inhibit the radial stretch-evoked responses described here. Furthermore, focal displacement has been found to elicit two distinct cationic conductances in different neuronal populations, one being sodium-selective and the other nonselective (14). The stretch-evoked

Data Analysis. Acquired images were displayed as the ratio of 340 nm to 380 nm and aligned using MetaMorph software. Cells were identified as neurons by eliciting depolarization with high potassium solution (75 mM) at the end of each experiment. Neurons were deemed to be stretch-sensitive if (i) the average of the first three points after stretch was >5 standard deviations above baseline intracellular calcium levels and (ii) post stimulus calcium level decayed back to baseline after stretch. Image analysis and statistics were done using Igor Pro (WaveMetrics). Movies were made using Adobe Photoshop and

MetaMorph. Statistical significance was assessed by one-way analysis of variance (ANOVA), followed by Tukey HSD.

ACKNOWLEDGMENTS. We thank Dr. Harlan Ives for providing generous access to the Flexcell system. This work was supported by predoctoral fellowships from the National Science Foundation (M.R.C.B. and H.H.), a Burroughs Wellcome Fund Career Award in Biomedical Sciences (D.M.B.), the Sandler Program in Basic Sciences (D.J. and E.A.L.), and the National Institutes of Health (D.J. and E.A.L.).

1. Garcia-Anoveros J, Corey DP (1997) The molecules of mechanosensation. *Annu Rev Neurosci* 20:567–594.
2. Gillespie PG, Walker RG (2001) Molecular basis of mechanosensory transduction. *Nature* 413:194–202.
3. Kung C (2005) A possible unifying principle for mechanosensation. *Nature* 436:647–654.
4. Lumpkin EA, Caterina MJ (2007) Mechanisms of sensory transduction in the skin. *Nature* 445:858–865.
5. Sukharev S, Corey DP (2004) Mechanosensitive channels: Multiplicity of families and gating paradigms. *Sci STKE* 2004 (219):re4.
6. Fields HL (1987) *Pain* (McGraw-Hill, New York) p 354.
7. Meyer R, Ringkamp M, Campbell J, Raja S (2006) Peripheral mechanisms of cutaneous nociception. *Textbook of Pain*, eds MacMahon S, Koltzenburg M (Elsevier/Churchill Livingstone, Philadelphia), 5th Ed, pp 3–34.
8. Koltzenburg M, Stucky CL, Lewin GR (1997) Receptive properties of mouse sensory neurons innervating hairy skin. *J Neurophysiol* 78:1841–1850.
9. Lewin GR, Moshourab R (2004) Mechanosensation and pain. *J Neurobiol* 61:30–44.
10. Kress M, Reeh PW (1996) More sensory competence for nociceptive neurons in culture. *Proc Natl Acad Sci USA* 93:14995–14997.
11. Alessandri-Haber N, et al. (2003) Hypotonicity induces TRPV4-mediated nociception in rat. *Neuron* 39:497–511.
12. Cho H, et al. (2006) A novel mechanosensitive channel identified in sensory neurons. *Eur J Neurosci* 23:2543–2550.
13. Cho H, Shin J, Shin CY, Lee SY, Oh U (2002) Mechanosensitive ion channels in cultured sensory neurons of neonatal rats. *J Neurosci* 22:1238–1247.
14. Drew LJ, Wood JN, Cesare P (2002) Distinct mechanosensitive properties of capsaicin-sensitive and -insensitive sensory neurons. *J Neurosci* 22:RC228.
15. Gotoh H, Takahashi A (1999) Mechanical stimuli induce intracellular calcium response in a subpopulation of cultured rat sensory neurons. *Neuroscience* 92:1323–1329.
16. Takahashi A, Gotoh H (2000) Mechanosensitive whole-cell currents in cultured rat somatosensory neurons. *Brain Res* 869:225–230.
17. Viana F, de la Pena E, Pecson B, Schmidt RF, Belmonte C (2001) Swelling-activated calcium signalling in cultured mouse primary sensory neurons. *Eur J Neurosci* 13:722–734.
18. Banes AJ, Gilbert J, Taylor D, Monbureau O (1985) A new vacuum-operated stress-providing instrument that applies static or variable duration cyclic tension or compression to cells in vitro. *J Cell Sci* 75:35–42.
19. Ito S, et al. (2008) A novel Ca²⁺ influx pathway activated by mechanical stretch in human airway smooth muscle cells. *Am J Respir Cell Mol Biol* 38:407–413.
20. Wirtz HR, Dobbs LG (1990) Calcium mobilization and exocytosis after one mechanical stretch of lung epithelial cells. *Science* 250:1266–1269.
21. Bautista DM, et al. (2008) Pungent agents from Szechuan peppers excite sensory neurons by inhibiting two-pore potassium channels. *Nat Neurosci* 11:772–779.
22. Julius D (2005) From peppers to peppermints: Natural products as probes of the pain pathway. *Harvey Lect* 101:89–115.
23. Bautista DM, et al. (2006) TRPA1 mediates the inflammatory actions of environmental irritants and proalgesic agents. *Cell* 124:1269–1282.
24. Jordt SE, et al. (2004) Mustard oils and cannabinoids excite sensory nerve fibres through the TRP channel ANKTM1. *Nature* 427:260–265.
25. McKemy DD, Neuhauser WM, Julius D (2002) Identification of a cold receptor reveals a general role for TRP channels in thermosensation. *Nature* 416:52–58.
26. Haeberle H, Bryan LA, Vadakkan TJ, Dickinson ME, Lumpkin EA (2008) Swelling-activated Ca²⁺ channels trigger Ca²⁺ signals in Merkel cells. *PLoS ONE* 3:e1750.
27. Liedtke WB, Heller S eds (2006) *TRP ion channel function in sensory transduction and cellular signaling cascades* (CRC Press, Boca Raton, FL), p 467.
28. Richard MN, Deniset JF, Kneesh AL, Blackwood D, Pierce GN (2007) Mechanical stretching stimulates smooth muscle cell growth, nuclear protein import, and nuclear pore expression through mitogen-activated protein kinase activation. *J Biol Chem* 282:23081–23088.